Spatio-temporal drivers of soil and ecosystem carbon fluxes at field scale in an upland grassland in Germany

Nils Borchard[1,4*], Michael Schirrmann[2], Christian von Hebel[1], Marius Schmidt[1], Roland Baatz[1], Les Firbank[3], Harry Vereecken[1], Michael Herbst[1]

[1] Agrosphere Institute (IBG-3), Jülich Research Centre, 52425 Jülich, Germany

[2] Leibniz Institute for Agricultural Engineering Potsdam-Bornim e.V., Max-Eyth-Allee 100, 14469 Potsdam, Germany

[3] School of Biology, University of Leeds, Leeds, LS2 9JT UK;

[4] Center for International Forestry Research, Jalan CIFOR, Situ Gede, Sindang Barang, Bogor 16115, Indonesia

*Corresponding author, N.Borchard@cgiar.org, Tel: ++62-251-8622676, Fax: ++62-251-8622100

Abstract

Ecosystem carbon (C) fluxes in terrestrial ecosystems are affected by varying environmental conditions (e.g. soil heterogeneity and the weather) and land management. However, the interactions between soil respiration (R_s) and net ecosystem exchange (NEE) and their spatio-temporal dependence on environmental conditions and land management at field scale is not well understood. We performed repeated C flux measurement at 21 sites during the 2013 growing season in a temperate upland grassland in Germany, which was fertilized and cut three times according to the agricultural practice typical of the region. Repeated measurements included determination of NEE, R_s, leaf area index (LAI), meteorological conditions as well as physical and chemical soil properties. Temporal variability of R_s was controlled by air temperature, while LAI influenced the temporal variability of NEE. The three grass cuts reduced LAI and affected NEE markedly. More than 50% of NEE variability was explained by defoliation at field scale. Additionally, soil heterogeneity affected NEE, but to a lower extent (>30%), while R_s remained unaffected. We conclude that grassland management (i.e. repeated defoliation) and soil heterogeneity affects the spatio-temporal variability of NEE at field scale.

Keywords: Net ecosystem exchange, Soil respiration, Grassland management, Leaf area index, Spatio-temporal variability, Field scale, Soil properties

1 Introduction

The interactions between environmental factors, including hydrological, meteorological and chemical conditions, and ecosystem carbon (C) fluxes have a profound influence on wider biogeochemical processes, yet they are not well understood (Chapin III *et al.*, 2009; Lohse *et al.*, 2009). While permanent grassland systems do not store as much carbon as forests, they are still potentially important in carbon cycles (Novick *et al.*, 2004; Scharlemann *et al.*, 2014). In Europe, more than 180 million ha (~34% of agricultural area) is occupied by permanent grassland (Smit *et al.*, 2008). In Central Europe (i.e. Atlantic Central Environmental Zone; Metzger *et al.*, 2005) upland temperate grassland ecosystems are characterized by mild temperatures and uniform precipitation over the growing season (i.e. 296 days with >10°C) that facilitates an annual grassland productivity of up to 7 t dry mass ha^{-1} (Dierschke and Briemle, 2002; Smit *et al.*, 2008). Thus, during the growing season, grass can be intensively managed and cut at least twice a year, promoting species such as *Lolium perenne* (Dierschke and Briemle, 2002; Pontes *et al.*, 2007). Beside biomass productivity and associated photosynthetic fixation of C in biomass, grassland ecosystems store large amounts of C in soils (Kuzyakov and Domanski, 2000; Guo and Gifford, 2002; Rees *et al.*, 2005).

Defoliation in terms of cutting and grazing may affect C fluxes and sequestration capabilities (Wan and Luo, 2003; Wohlfahrt *et al.*, 2008). Defoliation reduces leaf area, which affects photosynthesis and hydrocarbon allocation in plants as well as soil temperature and moisture (Wan *et al.*, 2002; Reichstein *et al.*, 2003; Wan and Luo, 2003; Carbone and Trumbore, 2007). This in turn reduces the capacity of grassland to capture C from atmosphere via photosynthesis while soil respiration (R_s) may be reduced or unaffected after defoliation (Bahn *et al.*, 2006; Bahn *et al.*, 2008), making the grassland a potential source of C. Several days after defoliation grassland may turn back into a net sink (Novick *et al.*, 2004; Zwicke *et al.*, 2013), as leaf area recovers, facilitating photosynthetic C assimilation that overcompensates the C release from the soil. Seasonal variability of precipitation, air temperature, and radiation also affects leaf area development and associated NEE (Suyker and Verma, 2001; Li *et al.*, 2005). Typically, high air temperatures are accompanied by high atmospheric vapor pressure deficits (VPD; i.e. low humidity), which affects stomata conductance (Buckley *et al.*, 2003; Klumpp *et al.*, 2007). The latter potentially limits photosynthesis if stomata are closed (Farquhar and Sharkey, 1982). Furthermore, radiation also affects NEE, due to the strong relation between photosynthetically active radiation (PAR) and photosynthesis (Gilmanov *et al.*, 2007; Chapin III *et al.*, 2011). In fact, numerous flux measurements revealed complex interactions between seasonally changing environmental factors (e.g. temperature, moisture etc.) and R_s as well as NEE (Reichstein *et al.*, 2003; Lasslop *et al.*, 2010). Yet, the relationships between NEE, site-specific variability of soil properties and vegetation have hardly been considered at field scale.

Since soil properties frequently vary considerably within distances shorter than 100 m in fields (Stutter *et al.*, 2009; Schirrmann and Domsch, 2011), the spatial pattern of plant performance and productivity (i.e. leaf area and photosynthetic activity) is equally complex (Ehrenfeld *et al.*, 2005; Krüger *et al.*, 2013). Additionally, R_s in grassland may correspond to daytime NEE (Gomez-Casanovas *et al.*, 2012), probably due to the rapid release of root exudates (e.g. easily decomposable carbohydrates) into the soil that fuel R_s (Kuzyakov and Domanski, 2000; Carbone and Trumbore, 2007). Carbon assimilation and transformation as well as C fluxes also respond to biogeochemical nutrient dynamics, soil physical properties, soil moisture and soil temperature (Raich and Tufekciogul, 2000; Fornara *et al.*, 2013), but their interactions and spatio-temporal dynamics that influence NEE at field scale remain unclear.

Therefore the aim of this study was to determine R_s and NEE variability at field scale in order to derive their spatio-temporal drivers. To this end, we established a net of 21 measurement sites and repeated C flux and LAI measurements weekly during the growing season in a permanent grassland in Rollesbroich (Germany). Additionally, chemical soil analyses and geophysical measurements were performed for all measurement sites. This approach allowed the assessment of *i)* the temporal effect of seasonally changing environmental drivers (i.e. temperature, soil moisture, PAR) and leaf area on R_s and NEE as well as *ii)* the spatio-temporal impact of spatially fragmented grassland management (i.e. different cutting regimes) and soil heterogeneity on spatial variability of R_s and NEE at field scale.

2 Material and methods

2.1 Site description and experimental design

The Rollesbroich test site is located in Germany (50°37' N, 6° 19' E; Figure 1) and includes an area of ~20 ha at altitudes ranging from 474 to 518 m a.s.l. The site is managed as permanent grassland (Montzka *et al.*, 2013); the fields are owned by different farmers using their own cutting and fertilizer regimes. The soils are dominated by (stagnic) Cambisols and Stagnosols on Devonian shales with occasional sandstone inclusions that are covered by a periglacial solifluction clay-silt layer of ~0.5 to 2 m thickness (Steffens, 2007). Bulk density increases from topsoil (0 to 5 cm: 0.79±0.02 g cm^{-3}) to subsoil (15 to 20 cm: 1.22±0.03 g cm^{-3}). Soil pH decreases from topsoil (0 to 5 cm; mean: 5.0, range: 4.8 to 5.3) to subsoil (15 to 20 cm; 4.9, range: 4.6 to 5.2). The mean annual air temperature and precipitation is 7.7°C and 1033 mm, respectively (Montzka *et al.*, 2013). Rollesbroich is included in the TERENO network of highly instrumented field sites (Zacharias *et al.*, 2011), providing soil moisture and soil temperature measured at soil depths of 5, 20 and 50 cm as well as precipitation, air temperature, PAR and VPD at a temporal resolution of 15 min (see also Material & Method section in Supplementary data).

To study the spatio-temporal patterns of C fluxes (i.e. R_s and NEE) at field scale, we performed a total of 412 repeated gas flux measurements as well as leaf area measurements at 21 sites (Figure 1, Table S-1, Supplementary data). In accordance with recent, local land management, all study sites were fertilized on 22nd March (18 m^3 biogas residues ha^{-1}; Möller and Müller, 2012) and grass was cut and harvested three times (Table S-1, Supplementary data). Further, to simulate the impact of different management strategies (i.e. cutting regimes) on C fluxes at the field scale, we split management sites alternately into two groups after day of year (DOY) 185 to establish plots (1 m^2) with two different cutting regimes (Table S-1, Supplementary data).

2.2 Gas flux and leaf area measurements

In April 2013, soil collars (polypropylene, 20 cm inner diameter) and soil frames (stainless steel, 1 m^2) to measure R_s and NEE, respectively, were installed in soil at each of the 21 measurement sites so that the upper edge protruded <3 cm above the mean soil surface and to facilitate land management (i.e. area restriction). Soil collars and frames were installed one month before the first measurements to minimize any disturbance effect (Prolingheuer *et al.*, 2014). Measurements started on DOY 120 and were repeated weekly until DOY 273, except for the calendar weeks 25 and 29 (see also Table S-2; Supplementary data). We restricted gas flux measurements at all 21 measurement sites to a tight schedule of 4 hours to minimize variation of PAR and temperature (Table S-2, Supplementary data).

Soil respiration was measured using a manual soil CO_2 flux chamber system (LI-8100 automated soil CO_2 flux system, LI-COR Inc., Lincoln, Nebraska, USA) in combination with an infra-red gas analyzer (IRGA) unit. Plants that grew inside soil collars were clipped to avoid bias due to aboveground vegetation (Johnson *et al.*, 2008; Wang *et al.*, 2013). The system used for closed chamber to determine NEE followed that of Langensiepen et al. (2012), connected to a LI-8100 unit (automated soil CO_2 flux system, LI-COR Inc., Lincoln, Nebraska, USA) and a temperature sensor (ETSS-HH thermocouple, Newport Electronics GmbH, Deckenpfronn, Germany). Briefly, the chamber had a basal area of a 1 m^2 and was adjustable on vegetation height plus an additional air space of 30 cm within closed cover on the top. Depending on growth stage, total volume ranged between 0.3 and 0.7 m^3. The chambers were made out of acrylic glass (Quinn-XT, Evonik Industries AG, Acrylic Polymers, Darmstadt, Germany) of 5 mm thickness with a range of heights (i.e. 10, 30 and 50cm). Further, to improve the homogeneity of the gas mixtures within the chambers, water-proof fans (Model IP 58, Conrad Elektronic SE, Hirschau, Germany) were installed in the top cover. Gas fluxes were derived from fitting a linear equation to CO_2 increase (2-s readings) during closure time using the LI-8100 file viewer application software (LI-COR FV8100, LI-COR Inc., version 3.1.0). Total (i.e. green plus brown) LAI was measured in triplicate using an optical plant canopy analyzer (LAI-2000, LI-COR Inc., Lincoln, Nebraska, USA).

2.3 Soil and vegetation survey, sampling and measurements

Soils were sampled in triplicate up to a depth of 20 cm at each of the 21 sites (Figure 1). Soil samples were analyzed for pH (VDLUFA, 1991c), concentrations of total C and nitrogen (N) as well as available potassium (K), magnesium (Mg) and phosphorous (P; VDLUFA, 1991b, a, e, d). Measured concentrations were converted to stocks by using measured soil bulk densities (see also Supplementary data).

Apparent electrical conductivity (EC_a) of soils was mapped up to a depth of 180 cm using electromagnetic induction (EMI) technology. In order to obtain spatial subsurface patterns, an EMI system was pulled by an all-terrain-vehicle at approximately 8 km/h over the test site while the measurements were geo-referenced and taken with a sampling rate of 10 Hz. Here, we used the CMD-MiniExplorer (GF-Instruments, Brno, Czech Republic) that provides six coil configurations since it houses one electromagnetic field transmitter and three receivers with 0.32, 0.71 and 1.18 m separation, which are oriented either vertical coplanar

(VCP) or horizontal coplanar (HCP). The VCP and HCP coil configurations are sensitive to shallow and deep subsurface material, respectively, and measure an apparent electrical conductivity (ECa) that is an mean value of overlapping sensing depths, called pseudo-depths (PD). To estimate the PD, the coil separation is multiplied by 0.75 and 1.5 for the VCP and HCP orientation, respectively (McNeill, 1980). Therefore, using the CMD-MiniExplorer, we recorded ECa values at six PD's, which were processed and interpolated as described by (von Hebel *et al.*, 2014). This resulted in six re-gridded spatially high resolution maps from which the ECa values, indicating changes with depth, were extracted at the respective measurement sites.

Detailed vegetation surveys were performed at three randomly selected sites (Figure 1; A, B, C; Table S-1; Supplementary data) on 7th May 2013 before the first grass cutting (Table S-1; Supplementary data). Higher plant species were identified in one pair of nested quadrats of 1 m^2 and 100 m^2 per survey site and cover by plants species was estimated for 1 m^2 plots using the Braun-Blanquet scale.

2.4 Data estimation and processing

Soil moisture and temperature at depths of 5, 20 and 50 cm were modelled by 3D-Kriging from the complete TERENO data sets. Prediction models were estimated on a daily basis considering each day as a single space-time model including all available measurement data that were sampled in a 15 minute time interval. A three-dimensional metric extension of the two-dimensional spatial plane was used considering the location as x, y and time as z for the use in 3D-Kriging. The axes x, y, and z were scaled in such a way that an isotropic semi-variogram model could be estimated from the empirical 3D semi-variogram. As semi-variogram model we used an exponential model type and fitted it with weighted least squares to the empirical 3D semi-variogram. Ordinary 3D block Kriging was used to predict soil moisture and temperature given the estimated semi-variogram parameters. The kriging block dimensions corresponded to point support in the x-y plane and to an hourly support along the z-axis, so that exactly at each measurement plot predicted soil temperature and soil moisture on an hourly basis was available.

Since photosynthesis is affected by vapor pressure and radiation (Farquhar and Sharkey, 1982; Buckley *et al.*, 2003; Zhang *et al.*, 2010) vapor pressure deficits and clear-sky indices (here the relative emissivity of long-wave radiation) were calculated prior to statistical evaluation. Vapor pressure deficit represents the saturated vapor pressure minus actual vapor pressure. Actual vapor pressure (VP_a [J m^{-3} that equals Pa]) was calculated as follows (Equation 1; Vaisala, 2013):

$$VP_a = \frac{A*T}{C}, \qquad \text{(Eq. 1)}$$

where *A* represents absolute humidity (g m^{-3}), *T* is air temperature (K) and *C* is a constant (2.16676 gK J^{-1}). Saturated vapor pressure was calculated using Equation 2, following Buck (1981):

$$VP_s = [(1.0007 + (3.46 * 10^{-6} * P)] * 6.1121 * e^{\frac{17.502*t}{240.97+t}}, \qquad \text{(Eq. 2)}$$

where *P* represents air pressure (hPa) and *t* air temperature (°C). Emissivity of solar radiation is explained by the Stefan-Boltzmann equation (Equation 3):

$$L = \varepsilon\sigma T^4, \qquad \text{(Eq. 3)}$$

where *L* is the incoming long-wave radiation for clear-sky conditions, *ε* is the clear-sky emissivity, and *T* is near-surface air temperature (K). The emissivity (ε) was determined using an algorithm (Equation 4) from Prata (1996), recommended by Flerchinger et al. (2009):

$$\varepsilon = 1 - \left(1 + \frac{4650*VP_a}{T}\right) exp\left\{-\left(1.2 + 3\,\frac{4650*VP_a}{T}\right)^{\frac{1}{2}}\right\}. \qquad \text{(Eq. 4)}$$

where VP_a is the actual vapor pressure (kPa) and T is near-surface air temperature (K). Finally, to assess a clear-sky index (k) previously computed long-wave radiation at clear-sky conditions (L) was related to incoming long-wave radiation (L_i, Equation 5) measured at the meteorological tower (NR01, Hukseflux Thermal Sensors, Delft, Netherlands):

$$k = \frac{L_i}{L}. \quad \text{(Eq. 5)}$$

Clear-sky conditions are indicated by k values equal or even larger than 1, which were used to identify net ecosystem measurements done at clear-sky conditions.

2.5 Statistical analyses

To reveal temporal interrelations between R_s, NEE, seasonally varying meteorological conditions and plant growth, we conducted a principal component analyses (PCA). The data sets included results of direct measurements (i.e. air temperature, precipitation, LAI, NEE, PAR and R_s) and processed values (i.e. VPD as well as soil moisture and soil temperature). Additionally, to assess the effect of cloudiness, PCAs were adapted to clear-sky conditions ($k \geq 1$ and $k < 1$). To avoid bias due to simulated cutting regimes established after DOY 185 we used data associated to initially established cutting regime (see above and Table S-1 & S-2; Supplementary data). Thus, only 292 measurements (i.e. total [412] – subsequently established cutting regime [120], Table S-2; Supplementary data; combination of LAI, NEE and R_s) were used to perform the principal component analyses. Data were tested for their normality using the Kolmogorov-Smirnov test and depending on their distribution, data were log or square-root transformed (Table 1). Finally we calculated z-scores and included variables with large communalities (>0.5) to facilitate Kaiser-Meyer-Olkin (KMO≥0.7) that maximized eligibility of correlation matrix and explained the variance of the extracted principle components using VARIMAX rotation.

To assess the effects of time (n=12), cutting regime (n=2) and soil heterogeneity on R_s and NEE, we performed repeated-measure general linear models (rGLM). We first categorized soil properties (n=21) into three units by using cluster analyses. Because there was no clear dependency between chemical soil properties and geo-physical soil properties, the data were split into *i)* chemical soil properties (i.e. soil acidity, C, K, Mg, N, P and soil depths) and *ii)* geo-physical soil properties (i.e. apparent electrical conductivity obtained by EMI) by using complete linkage clustering and Euclidian distances of z-transformed values. According to their distribution, grouped R_s and NEE values were logarithmic transformed before the rGLM procedures, which included the fixed effects of time, cutting regime and soil heterogeneity. Sphericity was tested using Machly's test and if sphericity was violated a Huynh-Feldt correction was used. Where *post hoc* pair-wise comparisons were made, the Fisher's Least significant difference test were used.

PCAs, rGLMs, and partial correlations were performed using SPSS (version 19, IBM Deutschland GmbH, Ehningen, Germany). For regression analysis and graphical representation, Sigma Plot 12 (SystatSoftware GmbH, Erkrath, Germany) was also used. Mean values are shown with their corresponding standard errors.

3 Results

3.1 Seasonal variability of meteorological conditions

Precipitation, air temperature, VPD and PAR followed a typical pattern during the measurement period (between DOY 91 to 273). Precipitation was 228.1 mm, with the minimum in May (0.9 mm) and maximum in June (89.8 mm; Figure 2). Air temperature was very low in April (mean: 6.1°C; range: -5.0°C to 21.4°C), but increased until July (mean: 17.2°C; range: 5.2°C to 28.6°C; Figure 2). Similarly, VPD was low in May (mean: 0.24 hPa) and increased until July (mean: 0.56 hPa). Clear-sky conditions were rare in May (Figure 2), which is reflected by lowest clear-sky indices (mean: 0.86). By contrast, highest clear-sky indices occurred in July (mean: 0.96). Depending on cloudiness and solar elevation angle (β), PAR was largest in July (mean: 479 µmol m^{-2} s^{-1}, maximum: 2153 µmol m^{-2} s^{-1}). Moreover, the temporal patterns of VPD and PAR were similar to those of air temperature, which explained 76% of VPD and 47% of PAR variability (VPD: $R^2_{exponential}$=0.76***; PAR: R^2_{linear}=0.47***).

Atmospheric conditions also affected soil conditions (e.g. moisture and temperature), soil respiration and water supply to plants. The soil moisture levels and temperatures determined for three soil depths (i.e. 5, 20 and 50 cm), followed the seasonal variability of atmospheric conditions. Thus, soil temperature at 5 cm initially showed low values in April with an mean of 6.2°C and a range between 0.2°C and 16.8°C, but increased until July to a mean of 17.3°C (range: 11.8°C to 23.7°C). Conversely, soil moisture increased from April (mean: 0.32 m^3 m^{-3}, range: 0.25 m^3 $m^{-3}$to 0.45 m^3 m^{-3}) to June (mean: 0.38 m^3 m^{-3}, range: 0.29 m^3 $m^{-3}$to 0.52 m^3 m^{-3}), but decreased sharply until August (mean: 0.25 m^3 m^{-3}, range: 0.23 m^3 $m^{-3}$to 0.28 m^3 m^{-3}).

3.2 Variation of soil and vegetation

The soils were classified as silty Cambisols, but soils varied spatially through weak stagnic properties and depth of developed B horizon, which reached a maximum 83 cm (mean: 58 cm, minimum: 36 cm).

Additionally, EMI measurements revealed the strongest variation of EC_a for deep soil layers with a pseudo-depth of 180 cm (coefficient of variation: 26%; mean: 2.3±0.1 mS m^{-1}), followed by a variability of 12% for the topsoil with a pseudo-depth of 25 cm (mean: -8.6±0.3 mS m^{-1}). The remaining four pseudo-depths in between 25 and 180 cm provided data that varied between -13.3±0.1 and 7.0 mS m^{-1}, but their variation ranged from 5% to 9%, respectively.

The soil contained varying amounts of organic C up to a depth of 20 cm ranging between 6.6 and 8.8 kg m^{-2} (mean: 7.8±0.1 kg m^{-2}). The latter indicates a relict plough horizon (A horizon mean depth: 19 cm, range: 13 cm to 27 cm). Additionally, soils to a depth of 20 cm contained varying stocks of total N (0.7 to 1.0 kg m^{-2}), available K (6.6 to 16.6 g m^{-2}), available Mg (16.3 to 30.9 g m^{-2}), and available P (2.9 to 7.7 g m^{-2}).

The major rooting zone was in the upper topsoil (0 to 5 cm) and contained more than 85±1 % (range: 72 to 96 %) of the total root biomass (i.e. live and dead roots; mean: 8.5±0.4 t ha^{-1}; range: 5.0 to 13.5 t ha^{-1}), which enabled plants to produce 5.8 to 7.9 t dry above ground biomass ha^{-1} (mean: 6.7±1.5 t ha^{-1}). Harvested above ground biomass contained on average 420.1±1.2 g C kg^{-1} dry mass and 21.9±0.6 g N kg^{-1} dry mass. The higher plant species composition was typical for traditionally managed grassland of the *Ranunculus repens-Alopecurus pratensis* plant community (Dierschke and Briemle, 2002; Table S-3, Supplementary data). Yet, abundance of major species (i.e. *Alopecurus pratensis, Lolium perenne, Poa trivialis* and *Rumex acetosa*) varied considerably (Table S-3; Supplementary data), which may affect at least spatial variability of R_s (Johnson *et al.*, 2008).

3.3 Soil respiration and net ecosystem exchange

Management strategies and soil heterogeneity had no effect on R_s in this study (Table 2), but variability of R_s significantly changed during the growing season (Table 2, Figure S-1, Supplementary data). High loadings of R_s, air temperature, VPD and PAR were seen in the principal component analysis (Figure 3, Table 3) indicating interactions among these variables (Figure 4). In detail, increased air temperature, PAR and VPD accelerated soil respiration following non-linear relations (Figure 4), but partial correlations revealed low dependency of VPD (r_p=-0.12*) as well as PAR (r_p=0.15**) on R_s at constant air temperature. Interestingly, soil temperature and soil moisture measured in three soil depths (i.e. 5 cm, 20 cm, and 50 cm) below extremely rooted upper topsoil (i.e. 0 to 5 cm) did not correlate with

R_s (Figure 3). Moreover, PCAs revealed that R_s and NEE were independent of each other, regardless of clear-sky conditions (Figure 3). NEE was also sensitive to time, management strategies and soil heterogeneity (Table 2, Figure 5). In this study, LAI over time varied with cutting (Figure 5) and greatly affected NEE following a non-linear relation (Figure 6).

4 Discussion

4.1 Interrelation between R_s, NEE, and seasonally varying meteorological conditions

Although, R_s in grassland may correlate with LAI and NEE (Bahn *et al.*, 2008; Gomez-Casanovas *et al.*, 2012), this study revealed no correlation between them. This corresponded with the results published by Bahn *et al.* (2006) that provided evidence of unaffected R_s after clipping (i.e. reduced LAI and NEE) due to mobilization of stored hydrocarbons. Regardless of the latter, our measurements revealed non-linear relation between R_s and meteorological conditions (i.e. air temperature, VPD, and PAR). Further, in line with existing literature (e.g. Lloyd and Taylor, 1994; Gomez-Casanovas *et al.*, 2013), measured R_s was related to air temperature following a non-linear relation, but not to soil temperature measured at 5 cm depths. Obviously, mean soil temperature in the extremely rooted upper topsoil (0 to 5 cm) was more related to air temperature due to limited thermal conductivity of this light and C enriched soil layer (0.79±0.02 g cm^{-3}, 47.6±1.1 g carbon kg^{-1}; Abu-Hamdeh and Reeder, 2000). Regardless of clear-sky conditions both VPD and PAR were related to R_s, which has rarely been described in literature (Kuzyakov and Gavrichkova, 2010; Cable *et al.*, 2013). In this study, R_s increased following a non-linear relation with increasing air temperature, PAR and VPD. However, air temperature explained the variability of VPD and PAR substantially. Air temperature may be the main controlling factor of R_s, which was confirmed by low partial correlations between R_s and VPD as well as PAR at constant air temperature. However, environmental conditions were sufficient to stimulate development of above ground biomass and formation of hydrocarbons as well as their translocation into roots and soil (i.e. release as exudates; Kuzyakov and Domanski, 2000; Carbone and Trumbore, 2007; Dieleman *et al.*, 2012) and probably soil respiration. Nevertheless, daytime R_s in the studied grassland was directly affected by air temperature and corresponding VPD and PAR that affected photosynthesis, and thus hydrocarbon supply into biologically most active soil layer.

Numerous studies revealed the strong non-linear relation between PAR and daytime NEE using the eddy covariance technique (Gilmanov *et al.*, 2007; Chapin III *et al.*, 2011). In our study NEE remained unaffected by PAR, most likely due to spatial variability of LAIs at field scale that overrode short-term variability of PAR (<4 hours; Table 1). Interestingly, LAI had a substantial effect on NEE in managed grassland, as also shown by Li *et al.* (2005) and Wohlfahrt *et al.* (2008), but even annual change of leaf area due to plant growth can affect NEE of natural grassland (Suyker and Verma, 2001; Chapin III *et al.*, 2009). Additionally, increasing VPD can reduce NEE due to stomata closure at soil water limited conditions (Novick *et al.*, 2004; Lasslop *et al.*, 2010). However, NEE was unaffected by VPD most likely due to sufficient water supply from soil. The latter was confirmed by soil water contents that were consistently >0.2 $m^3\ m^{-3}$, which allowed sufficient water-uptake through plants (Novick *et al.*, 2004; Ad-hoc-AG-Boden, 2005). This study showed that LAI was the major temporal driver of NEE and its variability.

4.2 Temporal and spatial pattern of carbon fluxes

R_s and NEE both varied with time with maximum values during most of the active growth period (Figure 6& 7). For R_s this pattern was in line with previous findings by Kreba *et al.* (2013) and Prolingheuer *et al.* (2014), who also revealed that temperature was major driver of temporal R_s variability. Furthermore, an additional driver of pronounced R_s during early growth period was an elevated allocation of newly formed hydrocarbons into roots (Carbone and Trumbore, 2007; Prolingheuer *et al.*, 2014), which may follow at each re-growth after defoliation. However, defoliation reduces hydrocarbon formation, which can decrease R_s for several days (Wan and Luo, 2003; Bahn *et al.*, 2008). Our finding revealed that defoliation hardly affected R_s, most likely due to elevated release of stored hydrocarbons that correlated to R_s (Fu and Cheng, 2004). NEE also peaked during the growing season with maximum values of -38.7 µmol m^{-2} s^{-1} at clear–sky conditions (i.e. day of year 185, mean: -27.7±1.5 µmol m^{-2} s^{-1}), which is clearly related to plant productivity and LAI (Flanagan *et al.*, 2002; Wohlfahrt *et al.*, 2008). Thus, different cutting regimes explained >50 % of total variability of NEE, which was induced by significant short-term changes of NEE that disappeared within 21 days in July and 14 days after cutting in August. Most likely, the rate of leaf area development after defoliation regulated the time required to restore NEE. Although reduced re-growth and leaf area development occurred after successive cuttings (Dierschke and Briemle, 2002; Wohlfahrt *et al.*, 2008), reduced soil moisture can decrease leaf area (Flanagan *et al.*, 2002). However, water was not a limiting factor, which was confirmed by soil water contents persistently >0.2 m^3 m^{-3} that provided sufficient water to plants.

Plant productivity is influenced by chemical and physical properties, that regulate water and nutrient supply to plants, while spatial heterogeneity of soil properties affects associations of plant species (Ehrenfeld *et al.*, 2005; Chapin III *et al.*, 2011; García-Palacios *et al.*, 2012). Whereas the chemical background of soil is caused by parent material, vegetation and human activity, the availability of water is governed by soil porosity and tortuosity (Lohse *et al.*, 2009) and meteorological conditions. Hence, separate assessments of varying soil properties at field scale obtained ex-situ (e.g. P, Mg, K, N, C, soil depth) and in-situ (EC_a) explained in each case >30 % of the general variability of NEE measurements, which provided evidence to upscale local NEE values up to field scale by using soil surveys or EC_a mappings. In fact, it might be promising to explore further the correlation of R_s and NEE with proximal soil sensing maps, because it will convey a more accurate image of the field scale variability into the models.

5 Conclusion

Our study confirmed that NEE in permanent grassland varied depending on seasonally changing LAI and grassland management at field scale (i.e. cutting regime). Defoliation reduced LAI of grasses, which in turn lowered NEE substantially. Moreover, defoliation has the potential to turn grassland into a net C-source, particularly if R_s remains unchanged. In our study, R_s was controlled by seasonally changing air temperature, while grassland management and soil heterogeneity hardly affected R_s during growth season. In contrast, soil heterogeneity modified NEE, but to a lower extent than repeated defoliation that explained more than 50% of NEE variability. Nevertheless, soil heterogeneity explained more than 30 % of NEE variability, which warrants upscaling of NEE measured at a particular location to spatial scales by using soil surveys or EC_a mappings. This study provided important insights in spatial and temporal variability of C fluxes in grassland, which may facilitate spatial partitioning of C-fluxes measured by eddy covariance at field scale in future studies.

Acknowledgment

This study was funded by the Deutsche Forschungsgesellschaft (DFG, SFB/TR 32 “Patterns in Soil-Vegetation-Atmosphere Systems: Monitoring, Modelling and Data Assimilation“), with vegetation data collection funded by the FP7 ExpeER project. In addition to the last, we thank the TERENO for providing meteorological and soil data. Many thanks are owed to the German Academic Exchange Service (DAAD) and International Association for the Exchange of Students for Technical Experience (IAESTE), for supporting students during their internships at the Forschungszentrum Jülich GmbH. Many thanks are owed to Dieter Wilden, the owner of the permanent grassland field in Rollesbroich (Germany), for the support during field work. Further we thank Silvia Siehoff for vegetation data collection and Holger Michler, Sandra Duarte Guardia, Sofia Elena Robles Arévalo, Haytham Qaddourah and Eser Güzel for assisting field measurements and their help with laboratory analyses.

References

Abu-Hamdeh, N.H., Reeder, R.C., 2000. Soil thermal conductivity effects of density, moisture, salt concentration, and organic matter. Soil Sci. Soc. Am. J., 1285-1290.

Ad-hoc-AG-Boden, 2005. Bodenkundliche Kartieranleitung (KA5). Schweizerbart'sche Verlagsbuchhandlung, Stuttgart, Germany.

Baatz, R., Bogena, H.R., Hendricks Franssen, H.J., Huisman, J.A., Qu, W., Montzka, C., Vereecken, H., 2014. Calibration of a catchment scale cosmic-ray probe network: A comparison of three parameterization methods. Journal of Hydrology doi: 10.1016/j.jhydrol.2014.02.026.

Bahn, M., Knapp, M., Garajova, Z., Pfahringer, N., Cernusca, A., 2006. Root respiration in temperate mountain grasslands differing in land use. Global Change Biology 12, 995-1006.

Bahn, M., Rodeghiero, M., Anderson-Dunn, M., Dore, S., Gimeno, C., Drosler, M., Williams, M., Ammann, C., Berninger, F., Flechard, C., Jones, S., Balzarolo, M., Kumar, S., Newesely, C., Priwitzer, T., Raschi, A., Siegwolf, R., Susiluoto, S., Tenhunen, J., Wohlfahrt, G., Cernusca, A., 2008. Soil respiration in european grasslands in relation to climate and assimilate supply. Ecosystems 11, 1352-1367.

Buck, A.L., 1981. New Equations for Computing Vapor Pressure and Enhancement Factor. Journal of Applied Meteorology 20, 1527-1532.

Buckley, T.N., Mott, K.A., Farquhar, G.D., 2003. A hydromechanical and biochemical model of stomatal conductance. Plant, Cell Environ. 26, 1767-1785.

Cable, J., Ogle, K., Barron-Gafford, G., Bentley, L., Cable, W., Scott, R., Williams, D., Huxman, T., 2013. Antecedent conditions influence soil respiration differences in shrub and grass patches. Ecosystems 16, 1230-1247.

Carbone, M.S., Trumbore, S.E., 2007. Contribution of new photosynthetic assimilates to respiration by perennial grasses and shrubs: residence times and allocation patterns. New Phytol. 176, 124-135.

Chapin III, F.S., Matson, P.A., Vitousek, P.M., 2011. Principles of terrestrial ecosystem ecology. Springer, Heidelberg, Germany.

Chapin III, F.S., McFarland, J., McGuire, A.D., Euskirchen, E.S., Ruess, R.W., Kielland, K., 2009. The changing global carbon cycle: linking plant–soil carbon dynamics to global consequences. J. Ecol. 97, 840-850.

Dieleman, W.I.J., Vicca, S., Dijkstra, F.A., Hagedorn, F., Hovenden, M.J., Larsen, K.S., Morgan, J.A., Volder, A., Beier, C., Dukes, J.S., King, J., Leuzinger, S., Linder, S., Luo, Y., Oren, R., De Angelis, P., Tingey, D., Hoosbeek, M.R., Janssens, I.A., 2012. Simple additive effects are rare: a quantitative review of plant biomass and soil process responses to combined manipulations of CO_2 and temperature. Global Change Biology 18, 2681-2693.

Dierschke, H., Briemle, G., 2002. Kulturgrasland: Wiesen, Weiden und verwandte Staudenfluren. Verlag Eugen Ulmer, Stuttgart, Germany.

Ehrenfeld, J., Ravit, B., Elgersma, K., 2005. Feedback in the plant-soil system. Annual Review of Environment and Resources 30, 75-115.

Farquhar, G.D., Sharkey, T.D., 1982. Stomatal conductance and photosynthesis. Annual Review of Plant Physiology 33, 317-345.

Flanagan, L.B., Wever, L.A., Carlson, P.J., 2002. Seasonal and interannual variation in carbon dioxide exchange and carbon balance in a northern temperate grassland. Global Change Biology 8, 599-615.

Flerchinger, G.N., Xaio, W., Marks, D., Sauer, T.J., Yu, Q., 2009. Comparison of algorithms for incoming atmospheric long-wave radiation. Water Resources Research 45, W03423.

Fornara, D.A., Banin, L., Crawley, M.J., 2013. Multi-nutrient vs. nitrogen-only effects on carbon sequestration in grassland soils. Global Change Biology 19, 3848-3857.

Fu, S., Cheng, W., 2004. Defoliation affects rhizosphere respiration and rhizosphere priming effect on decomposition of soil organic matter under a sunflower species: *Helianthus annuus*. Plant Soil 263, 345-352.

García-Palacios, P., Maestre, F.T., Bardgett, R.D., de Kroon, H., 2012. Plant responses to soil heterogeneity and global environmental change. J. Ecol. 100, 1303-1314.

Gilmanov, T.G., Soussana, J.E., Aires, L., Allard, V., Ammann, C., Balzarolo, M., Barcza, Z., Bernhofer, C., Campbell, C.L., Cernusca, A., Cescatti, A., Clifton-Brown, J., Dirks, B.O.M., Dore, S., Eugster, W., Fuhrer, J., Gimeno, C., Gruenwald, T., Haszpra, L., Hensen, A., Ibrom, A., Jacobs, A.F.G., Jones, M.B., Lanigan, G., Laurila, T., Lohila, A., Manca, G., Marcolla, B., Nagy, Z., Pilegaard, K., Pinter, K., Pio, C., Raschi, A., Rogiers, N., Sanz, M.J., Stefani, P., Sutton, M., Tuba, Z., Valentini, R., Williams, M.L., Wohlfahrt, G., 2007. Partitioning European grassland net ecosystem CO_2 exchange into gross primary productivity and ecosystem respiration using light response function analysis. Agric., Ecosyst. Environ. 121, 93-120.

Gomez-Casanovas, N., Anderson-Teixeira, K., Zeri, M., Bernacchi, C.J., DeLucia, E.H., 2013. Gap filling strategies and error in estimating annual soil respiration. Global Change Biology 19, 1941-1952.

Gomez-Casanovas, N., Matamala, R., Cook, D.R., Gonzalez-Meler, M.A., 2012. Net ecosystem exchange modifies the relationship between the autotrophic and heterotrophic components of soil respiration with abiotic factors in prairie grasslands. Global Change Biology 18, 2532-2545.

Guo, L.B., Gifford, R.M., 2002. Soil carbon stocks and land use change: a meta analysis. Global Change Biology 8, 345-360.

Johnson, D., Phoenix, G.K., Grime, J.P., 2008. Plant community composition, not diversity, regulates soil respiration in grasslands. Biol. Lett. 4, 345-348.

Klumpp, K., Soussana, J.F., Falcimagne, R., 2007. Effects of past and current disturbance on carbon cycling in grassland mesocosms. Agric., Ecosyst. Environ. 121, 59-73.

Kreba, S.A., Coyne, M.S., McCulley, R.L., Wendroth, O.O., 2013. Spatial and temporal patterns of carbon dioxide flux in crop and grass land-use systems. Vadose Zone J., doi: 10.2136/vzj2013.2101.0005.

Krüger, J., Franko, U., Fank, J., Stelzl, E., Dietrich, P., Pohle, M., Werban, U., 2013. Linking geophysics and soil function modeling - An application study for biomass production. Vadose Zone Journal, doi: 10.2136/vzj2013.2101.0015.

Kuzyakov, Y., Domanski, G., 2000. Carbon input by plants into the soil. Review. J. Plant Nutr. Soil Sci. 163, 421-431.

Kuzyakov, Y., Gavrichkova, O., 2010. Time lag between photosynthesis and carbon dioxide efflux from soil: a review of mechanisms and controls. Global Change Biology 16, 3386-3406.

Langensiepen, M., Kupisch, M., van Wijk, M.T., Ewert, F., 2012. Analyzing transient closed chamber effects on canopy gas exchange for optimizing flux calculation timing. Agric. For. Meteorol. 164, 61-70.

Lasslop, G., Reichstein, M., Papale, D., Richardson, A.D., Arneth, A., Barr, A., Stoy, P., Wohlfahrt, G., 2010. Separation of net ecosystem exchange into assimilation and respiration using a light response curve approach: critical issues and global evaluation. Global Change Biology 16, 187-208.

Levine, T.R., Hullett, C.R., 2002. Eta squared, partial eta squared, and misreporting of effect size in communication research. Human Communication Research 28, 612-625.

Li, S.G., Asanuma, J., Eugster, W., Kotani, A., Liu, J.J., Urano, T., Oikawa, T., Davaa, G., Oyunbaatar, D., Sugita, M., 2005. Net ecosystem carbon dioxide exchange over grazed steppe in central Mongolia. Global Change Biology 11, 1941-1955.

Lloyd, J., Taylor, J.A., 1994. On the temperature-dependence of soil respiration. Funct. Ecol. 8, 315-323.

Lohse, K.A., Brooks, P.D., McIntosh, J.C., Meixner, T., Huxman, T.E., 2009. Interactions between biogeochemistry and hydrologic systems. Annual Review of Environment and Resources 34, 65-96.

McNeill, J.D., 1980. Electromagnetic terrain conductivity measurement at low induction numbers. Technical Note TN-6. Geonics Ltd., Mississauga, Ontario, Canada

Metzger, M.J., Bunce, R.G.H., Jongman, R.H.G., Mücher, C.A., Watkins, J.W., 2005. A climatic stratification of the environment of Europe. Global Ecol. Biogeogr. 14, 549-563.

Möller, K., Müller, T., 2012. Effects of anaerobic digestion on digestate nutrient availability and crop growth: A review. Eng. Life Sci. 12, 242-257.

Montzka, C., Bogena, H.R., Weihermuller, L., Jonard, F., Bouzinac, C., Kainulainen, J., Balling, J.E., Loew, A., dall'Amico, J.T., Rouhe, E., Vanderborght, J., Vereecken, H., 2013. Brightness temperature and soil moisture validation at different scales during the SMOS validation campaign in the Rur and Erft catchments, Germany. Geoscience and Remote Sensing, IEEE Transactions on 51, 1728-1743.

Novick, K.A., Stoy, P.C., Katul, G.G., Ellsworth, D.S., Siqueira, M.B.S., Juang, J., Oren, R., 2004. Carbon dioxide and water vapor exchange in a warm temperate grassland. Oecologia 138, 259-274.

Pontes, L.S., Carrère, P., Andueza, D., Louault, F., Soussana, J.F., 2007. Seasonal productivity and nutritive value of temperate grasses found in semi-natural pastures in Europe: responses to cutting frequency and N supply. Grass Forage Sci. 62, 485-496.

Prata, A.J., 1996. A new long-wave formula for estimating downward clear-sky radiation at the surface. Quarterly Journal of the Royal Meteorological Society 122, 1127-1151.

Prolingheuer, N., Scharnagl, B., Graf, A., Vereecken, H., Herbst, M., 2014. On the spatial variation of soil rhizospheric and heterotrophic respiration in a winter wheat stand. Agric. For. Meteorol. 195–196, 24-31.

Raich, J., Tufekciogul, A., 2000. Vegetation and soil respiration: Correlations and controls. Biogeochemistry 48, 71-90.

Rees, R.M., Bingham, I.J., Baddeley, J.A., Watson, C.A., 2005. The role of plants and land management in sequestering soil carbon in temperate arable and grassland ecosystems. Geoderma 128, 130-154.

Reichstein, M., Rey, A., Freibauer, A., Tenhunen, J., Valentini, R., Banza, J., Casals, P., Cheng, Y., Grünzweig, J.M., Irvine, J., Joffre, R., Law, B.E., Loustau, D., Miglietta, F., Oechel, W., Ourcival, J.-M., Pereira, J.S., Peressotti, A., Ponti, F., Qi, Y., Rambal, S., Rayment, M., Romanya, J., Rossi, F., Tedeschi, V., Tirone, G., Xu, M., Yakir, D., 2003. Modeling temporal and large-scale spatial variability of soil respiration from soil water availability, temperature and vegetation productivity indices. Glob. Biogeochem. Cycle 17, 1104.

Scharlemann, J.P.W., Tanner, E.V.J., Hiederer, R., Kapos, V., 2014. Global soil carbon: understanding and managing the largest terrestrial carbon pool. Carbon Management 5, 81-91.

Schirrmann, M., Domsch, H., 2011. Sampling procedure simulating on-the-go sensing for soil nutrients. J. Plant Nutr. Soil Sci. 174, 333-343.

Smit, H.J., Metzger, M.J., Ewert, F., 2008. Spatial distribution of grassland productivity and land use in Europe. Agricultural Systems 98, 208-219.

Steffens, W., 2007. Bodenkarte zur Standorterkundung, Verfahren: Rollesbroich (Landwirtschaft), 1:2.500. Geologischer Dienst Nordrhein-Westfalen, Krefeld.

Stutter, M.I., Lumsdon, D.G., Billett, M.F., Low, D., Deeks, L.K., 2009. Spatial variability in properties affecting organic horizon carbon storage in upland soils. Soil Sci. Soc. Am. J., 1724-1732.

Suyker, A.E., Verma, S.B., 2001. Year-round observations of the net ecosystem exchange of carbon dioxide in a native tallgrass prairie. Global Change Biology 7, 279-289.

Vaisala, 2013. Humidity conversion formulas: Calculation formulars for humidity. Helsinki, Finland, p. 16.

VDLUFA, 1991a. A 2.2.5 Verbrennung und Gasanalyse (nach DUMAS). In: Landwirtschaftlicher, V.D., (VDLUFA), U.-u.F.e.V. (Eds.), Handbuch der

Landwirtschaftlichen Versuchs- und Untersuchungsmethodik (VDLUFA-Handbuch), Band I Die Untersuchung von Böden. VDLUFA-Verlag, Darmstadt.

VDLUFA, 1991b. A 4.1.3.1 Differenz aus Gesamt-Kohlenstoff nach Verbrennung und Gasanalyse und anorganischem Kohlenstoff. In: Landwirtschaftlicher, V.D., (VDLUFA), U.-u.F.e.V. (Eds.), Handbuch der Landwirtschaftlichen Versuchs- und Untersuchungsmethodik (VDLUFA-Handbuch), Band I Die Untersuchung von Böden. VDLUFA-Verlag, Darmstadt.

VDLUFA, 1991c. A 5.1.1 pH-Wert. In: Landwirtschaftlicher, V.D., (VDLUFA), U.-u.F.e.V. (Eds.), Handbuch der Landwirtschaftlichen Versuchs- und Untersuchungsmethodik (VDLUFA-Handbuch), Band I Die Untersuchung von Böden. VDLUFA-Verlag, Darmstadt.

VDLUFA, 1991d. A 6.2.1.1 Phosphor und Kalium, CAL-Auszug. In: Landwirtschaftlicher, V.D., (VDLUFA), U.-u.F.e.V. (Eds.), Handbuch der Landwirtschaftlichen Versuchs- und Untersuchungsmethodik (VDLUFA-Handbuch), Band I Die Untersuchung von Böden. VDLUFA-Verlag, Darmstadt.

VDLUFA, 1991e. A 6.2.4.1 Calciumchloridauszug. In: Landwirtschaftlicher, V.D., (VDLUFA), U.-u.F.e.V. (Eds.), Handbuch der Landwirtschaftlichen Versuchs- und Untersuchungsmethodik (VDLUFA-Handbuch), Band I Die Untersuchung von Böden. VDLUFA-Verlag, Darmstadt.

von Hebel, C., Rudolph, S., Mester, A., Huisman, J.A., Kumbhar, P., Vereecken, H., van der Kruk, J., 2014. Three-dimensional imaging of subsurface structural patterns using quantitative large-scale multiconfiguration electromagnetic induction data. Water Resources Research 50, 2732-2748.

Wan, S., Luo, Y., 2003. Substrate regulation of soil respiration in a tallgrass prairie: Results of a clipping and shading experiment. Global Biogeochem. Cycles 17, 1054.

Wan, S., Luo, Y., Wallace, L.L., 2002. Changes in microclimate induced by experimental warming and clipping in tallgrass prairie. Global Change Biology 8, 754-768.

Wang, W., Zeng, W., Chen, W., Zeng, H., Fang, J., 2013. Soil respiration and organic carbon dynamics with grassland conversions to woodlands in temperate China. PLoS ONE 8, e71986.

Wohlfahrt, G., Anderson-Dunn, M., Bahn, M., Balzarolo, M., Berninger, F., Campbell, C., Carrara, A., Cescatti, A., Christensen, T., Dore, S., Eugster, W., Friborg, T., Furger, M., Gianelle, D., Gimeno, C., Hargreaves, K., Hari, P., Haslwanter, A., Johansson, T., Marcolla, B., Milford, C., Nagy, Z., Nemitz, E., Rogiers, N., Sanz, M.J., Siegwolf, R.T.W., Susiluoto, S., Sutton, M., Tuba, Z., Ugolini, F., Valentini, R., Zorer, R., Cernusca, A., 2008. Biotic, abiotic, and management controls on the net ecosystem CO_2 exchange of European mountain grassland ecosystems. Ecosystems 11, 1338-1351.

Zacharias, S., Bogena, H., Samaniego, L., Mauder, M., Fuß, R., Pütz, T., Frenzel, M., Schwank, M., Baessler, C., Butterbach-Bahl, K., Bens, O., Borg, E., Brauer, A., Dietrich, P., Hajnsek, I., Helle, G., Kiese, R., Kunstmann, H., Klotz, S., Munch, J.C., Papen, H., Priesack, E., Schmid, H.P., Steinbrecher, R., Rosenbaum, U., Teutsch, G., Vereecken, H., 2011. A network of terrestrial environmental observatories in Germany. Vadose Zone J., 955-973.

Zhang, M., Yu, G.R., Zhang, L.M., Sun, X.M., Wen, X.F., Han, S.J., Yan, J.H., 2010. Impact of cloudiness on net ecosystem exchange of carbon dioxide in different types of forest ecosystems in China. Biogeosciences 7, 711-722.

Zwicke, M., Alessio, G.A., Thiery, L., Falcimagne, R., Baumont, R., Rossignol, N., Soussana, J.-F., Picon-Cochard, C., 2013. Lasting effects of climate disturbance on perennial grassland above-ground biomass production under two cutting frequencies. Global Change Biology 19, 3434-3448.

603

Table 1: In-field and laboratory determined variables that were used for principal component analyses. Non-normal distributed data were transformed according to their distribution. Total variation represents absolute coefficient of variance (%) of all measurement (n=412) while daily variation shows mean absolute variation (%) and their standard error of measurements of each single day (measurement time was restricted to 4 hours). Since air temperature affected soil respiration significantly (Figure 4) soil respiration data were de-trended, which reduced variability (shown in parenthesis).

Variable	Unit	Method/Source	Transformation	Total variation	Daily variation
Net ecosystem exchange	$\mu mol\ m^{-2}\ s^{-1}$	IRGA	-/-	90	7.6±3.9
Total soil respiration	$\mu mol\ m^{-2}\ s^{-1}$	IRGA	-/-	35 (19)	4.4±0.5 (0.7±0.1)
Photosynthetically active radiation	$\mu mol\ m^{-2}\ s^{-1}$	Qantum PAR sensor	-/-	56	6.6±0.9
Leaf area index	$m^2\ m^{-2}$	Plant canopy analyzer	Log-transformed	76	8.8±1.0
Vapor pressure deficit[†]	hPa	-/-	Log-transformed	82	6.7±1.3
Air temperature[†]	°C	Temperature probe	-/-	39	1.8±0.3
Soil temperature in 5 cm[‡]	°C	TERENO	-/-	20	1.1±0.1
Soil temperature in 20 cm[‡]	°C	TERENO	Sqrt-transformed	19	0.9±0.2
Soil temperature in 50 cm[‡]	°C	TERENO	Log-transformed	19	0.9±0.0
Soil water content in 5 cm[‡]	$cm^3\ cm^{-3}$	TERENO	Sqrt-transformed	32	0.0±0.0
Soil water content in 20 cm[‡]	$cm^3\ cm^{-3}$	TERENO	Sqrt-transformed	22	2.0±0.2
Soil water content in 50 cm[‡]	$cm^3\ cm^{-3}$	TERENO	Sqrt-transformed	19	3.3±0.2

† Data were calculated; see also Material and Method section in Supplementary data.

‡ Data were predicted by 3D-Kriging from complete TERENO data sets (see Material & Method section in Supplementary data).

IRGA: infrared gas analyzer; PAR: photosynthetically active radiation; TERENO: Terrestrial Environmental Observatories; Log: logarithm; Sqrt: square root

Table 2: Percentage of total variability (μ_p^2) of NEE and soil respiration attributable to time, management strategies, and spatial pattern of soil properties as well as soil pattern obtained by electromagnetic induction (EMI) measurements on repeated measurements of net ecosystem exchange and de-trended soil respiration. Net ecosystem exchange and soil respiration data were log-transformed prior statistical evaluation. F-statistics are shown.

Factor	Net ecosystem exchange		De-trended total soil respiration	
	Soil properties	EMI pattern	Soil properties	EMI pattern
	μ_p^2	μ_p^2	μ_p^2	μ_p^2
The time hypothesis: Do time and its interaction terms cause variability on C-fluxes (i.e. within-subject effects)?				
T	63*** $_{F(10,155)=25.1}$	56*** $_{F(10,153)=18.8}$	96*** $_{F(2,33)=371.2}$	95*** $_{F(2,36)=295.3}$
T x MT	46*** $_{F(10,155)=13.0}$	35*** $_{F(10,153)=8.2}$	1 $_{F(2,33)=0.2}$	3 $_{F(2,36)=0.4}$
T x SP	25** $_{F(21,155)=2.5}$	17 $_{F(20,153)=1.5}$	22 $_{F(4,33)=2.1}$	9 $_{F(5,36)=0.7}$
T x MT x SP	22** $_{F(21,155)=2.1}$	13 $_{F(20,153)=1.1}$	11 $_{F(4,33)=0.5}$	15 $_{F(5,36)=1.3}$
The individual factor hypothesis: Do individual factors affect variability of C-fluxes (i.e. between-subject effects)?				
MT	52** $_{F(1,15)=16.4}$	51** $_{F(1,15)=15.5}$	1 $_{F(1,15)=0.1}$	2 $_{F(1,15)=0.2}$
SP	33* $_{F(2,15)=3.7}$	38* $_{F(2,15)=4.5}$	7 $_{F(2,15)=0.7}$	13 $_{F(2,15)=1.1}$
MT x SP	9 $_{F(2,15)=0.7}$	8 $_{F(2,15)=0.7}$	6 $_{F(2,15)=0.7}$	11 $_{F(2,15)=0.9}$

T time, i.e. repeated measurements

MT management regime, i.e. cutting regime

SP spatial pattern of included soil properties i.e. stocks of P, Mg, K, N, C and acidity (i.e. concentration of H^+ calculated from pH) within soil up to depth of 20 cm plus soil depths of developed A and B horizon

Electromagnetic induction measurements were measurements of apparent electrical conductivity

Effect size is represents by partial eta-square (μ_p^2) that describes proportion of total variability attributable to a factor (Levine and Hullett, 2002).

Asterisks indicate different probability levels: *** $P<0.001$, ** $P<0.01$, * $P<0.05$

Table 3: Results from PCAs; their variable loadings and explained variability of each principal component.

	Principal components									
	All sky conditions				Clear-sky conditions			Non-clear-sky conditions		
	1	2	3	4	1	2	3	1	2	3
Net ecosystem exchange	-.159	.112	-.003	**-.876**	-.120	.205	**.877**	-.416	.152	**-.796**
Soil respiration	**.770**	.193	.112	.172	-.032	**.928**	-.135	**.786**	.177	.039
Photo-synthetically active radiation	**.879**	.004	-.108	-.082	.028	**.933**	.102	**.846**	-.052	.223
Air temperature	**.805**	.449	-.232	-.094	**.781**	**.561**	.065	**.837**	.448	-.120
Vapor pressure deficit	**.883**	.042	-.278	-.172	**.622**	**.675**	.333	**.898**	.001	-.181
Leaf area index	-.307	.189	.021	**.837**	.223	.180	**-.883**	-.140	.208	**.838**
Soil temperature (5cm)	.337	**.880**	-.119	.109	**.879**	.152	-.241	.435	**.856**	.012
Soil temperature (20cm)	.075	**.890**	-.229	.142	**.903**	-.145	-.318	.188	**.914**	.055
Soil temperature (50cm)	.035	**.810**	-.285	-.186	ex.	ex.	ex.	-.151	**.884**	-.073
Soil water content (5cm)	-.266	-.325	**.616**	.237	**-.725**	-.374	.187	ex.	ex.	ex.
Soil water content (20cm)	-.199	-.189	**.763**	.095	**-.902**	.209	.039	-.360	-.196	.409
Soil water content (50cm)	.050	-.145	**.742**	-.182	ex.	ex.	ex.	ex.	ex.	ex.
Explained variability (%)	26.2	22.3	15.1	14.2	39.9	28.0	18.9	34.1	26.9.	16.1

ex.: Data were excluded from PCA to increase Kaiser-Meyer-Olkin criteria

Figure 1: The Rollesbroich test site where repeated carbon flux and leaf area measurements were performed at 21 measurement sites in a permanent grassland. This site is part of the TERENO project and provides framework for the installed 188 SoilNet sensor units that measure soil temperature and soil moisture at soil depths of 5 cm, 20 cm and 50 cm (Baatz *et al.*, 2014). Near measurement site number 20, meteorological conditions (i.e. air temperature, precipitation, photosynthetically active radiation and vapor pressure) are continuously measured with a temporal resolution of 10 min. At sites A, B and C vegetation was surveyed. Soils differed in thickness of periglacial solifluction clay-silt layer with moderate to (max. 60 cm) deep layers (max. 100 cm; Steffens, 2007).

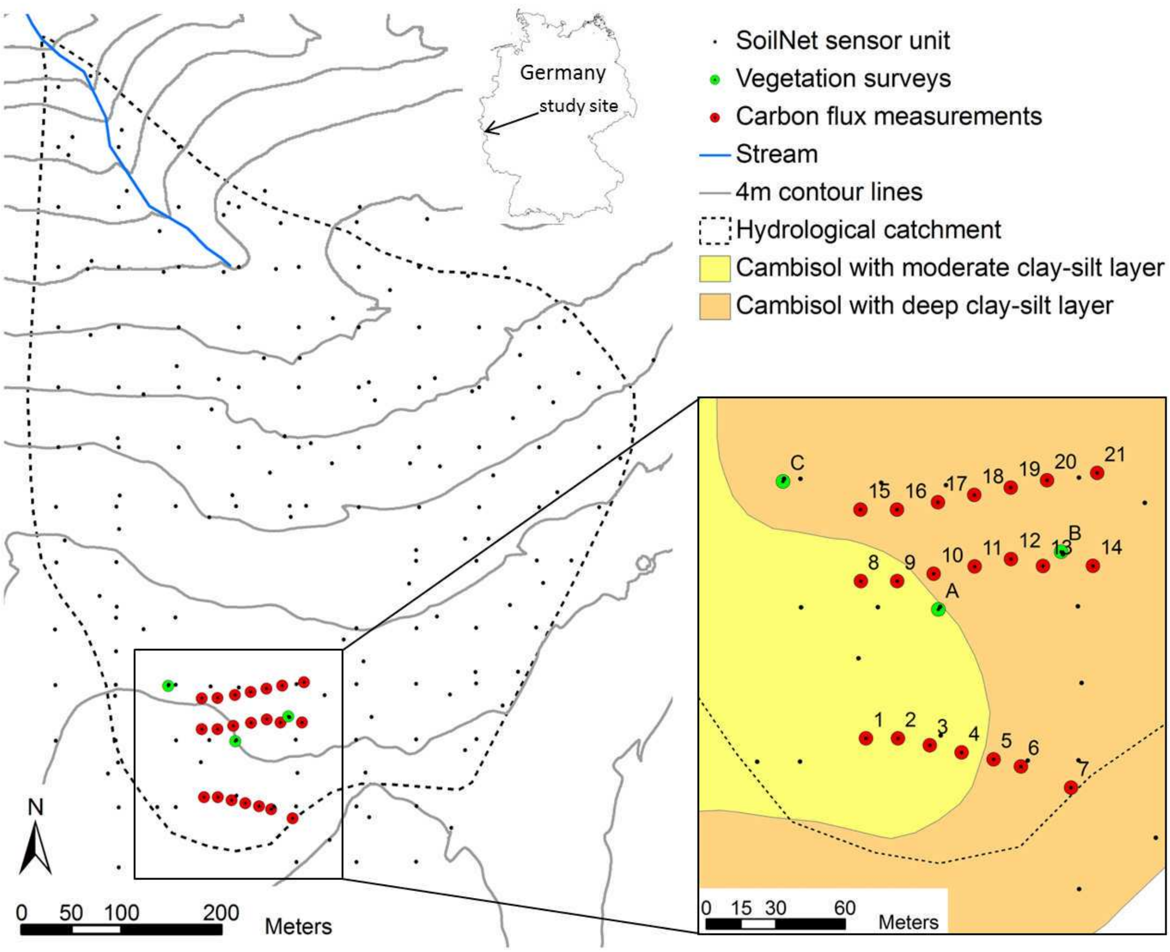

Figure 2: Meteorological data measured during measurement campaign in 2013. Precipitation is shown on daily resolution, while air temperature, vapor pressure deficit (VPD), photosynthetically active radiation (PAR) and calculated clear-sky index (CI) are presented on hourly resolution.

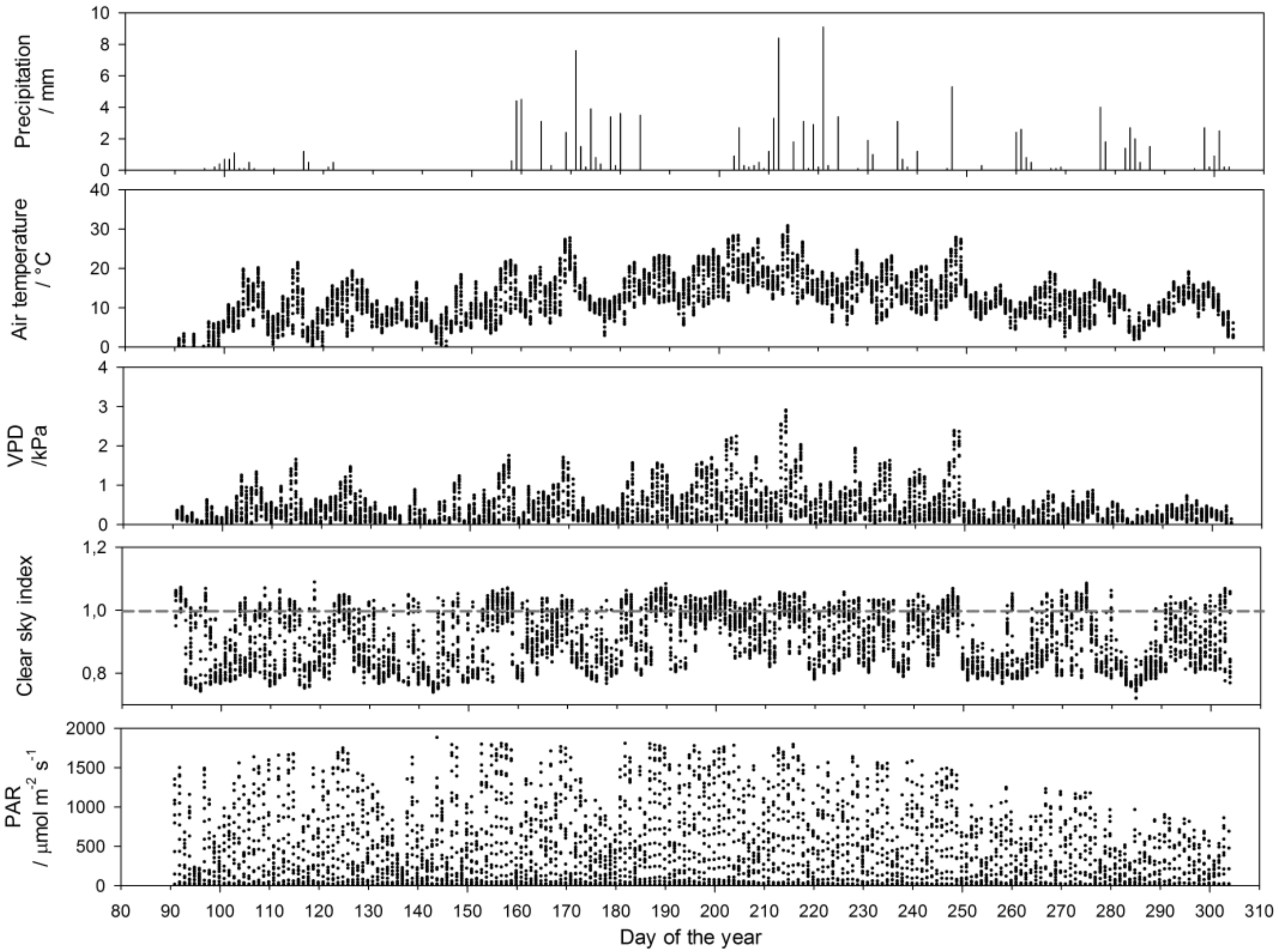

Figure 3: Correlations between loadings and principal components based on measurements performed on sites with management strategy X (Table S-1, Supplementary data; after DOY 185 we split plots regarding cutting regime performed by local farmers into plots with cutting regime X and Y, see also Table S-2; Supplementary data) of net ecosystem exchange (NEE), total soil respiration (Rs), leaf area index (LAI), photosynthetically active radiation (PAR), air temperature (T_{Air}), vapor pressure deficit (VPD) and soil moisture (SWC) as well as temperature (T) at three soil depths (5 cm, 20 cm, 50 cm). Principal component analysis was performed using all measurements that were related to management strategy X (n = 292), which includes 203 measurements done at non-clear-sky conditions and 89 measurements done at clear-sky conditions. PC = principal component, with explained variance in parentheses.

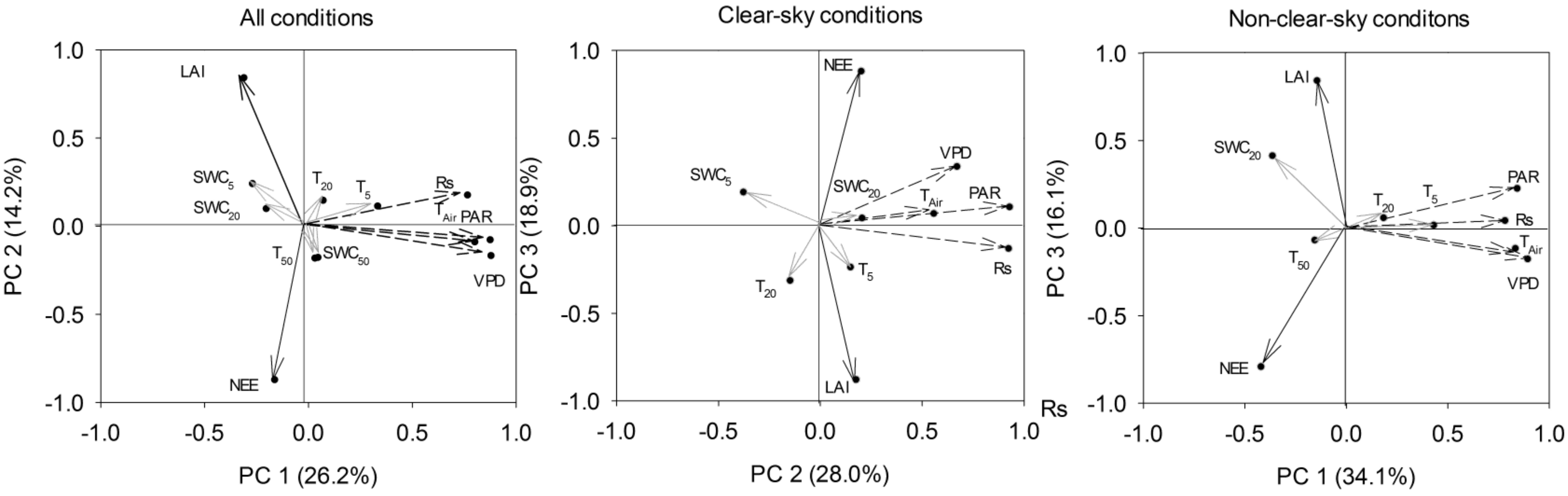

Figure 4: Relation between soil respiration and air temperature (Figure 4.a), vapor pressure deficit (Figure 4.b) as well as photosynthetically active radiation (Figure 4.c). Data sets include values obtained at all 21 measurement sites where management strategy X was established (n=292; Table S-2, Supplementary data). Best fits are shown as solid line and respective equations are provided.

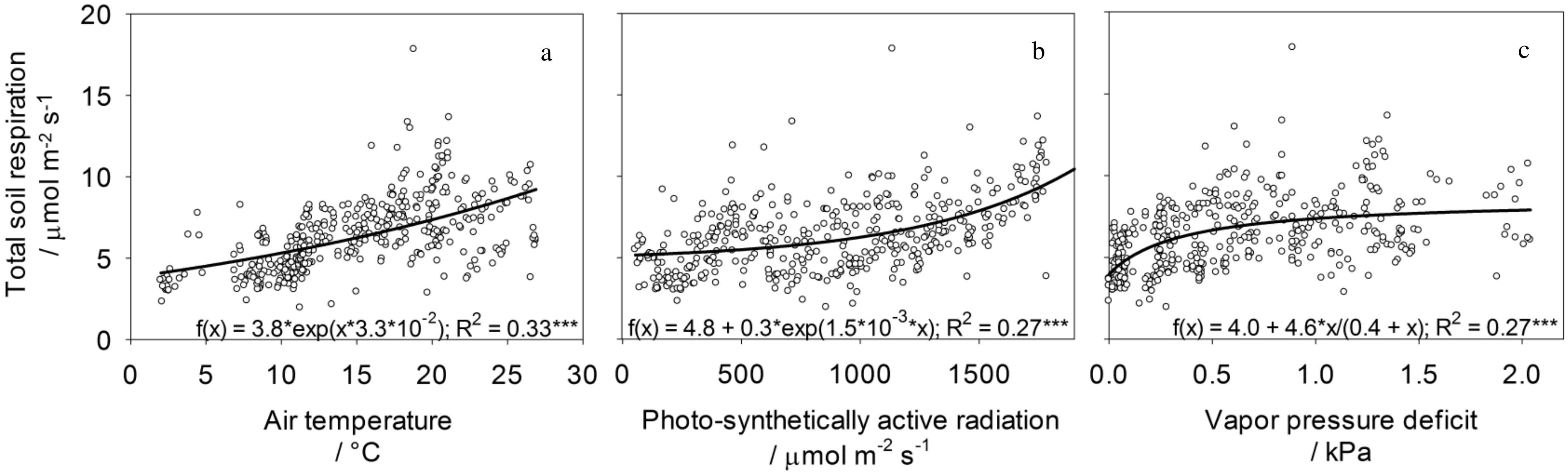

Figure 5: Effect of different grassland management strategies (i.e. cutting regime, Table S-1: Supplementary data) on net ecosystem exchange and leaf area index and their relative values $\left[Change(\%) = \left[\frac{(management\ strategy\ X - management\ strategy\ Y)}{management\ strategy\ Y}\right] * 100\right]$. Until day 185 all sites were managed similarly, thereafter grass from 10 sitens was cut later to simulate management strategy Y performed by another farmer (Table S-1 and S-2, Supplementary data). Significant differences (Mann-Whitney-U test of non-transformed data) of net ecosystem exchange are indicated with asterisks (i.e. * P<0.05; ** P>0.01; *** P>0.001) and those of leaf area indices are shown with hash mark (.e. # P<0.05; ## P>0.01; ### P>0.001). Lines are visual aids.

662

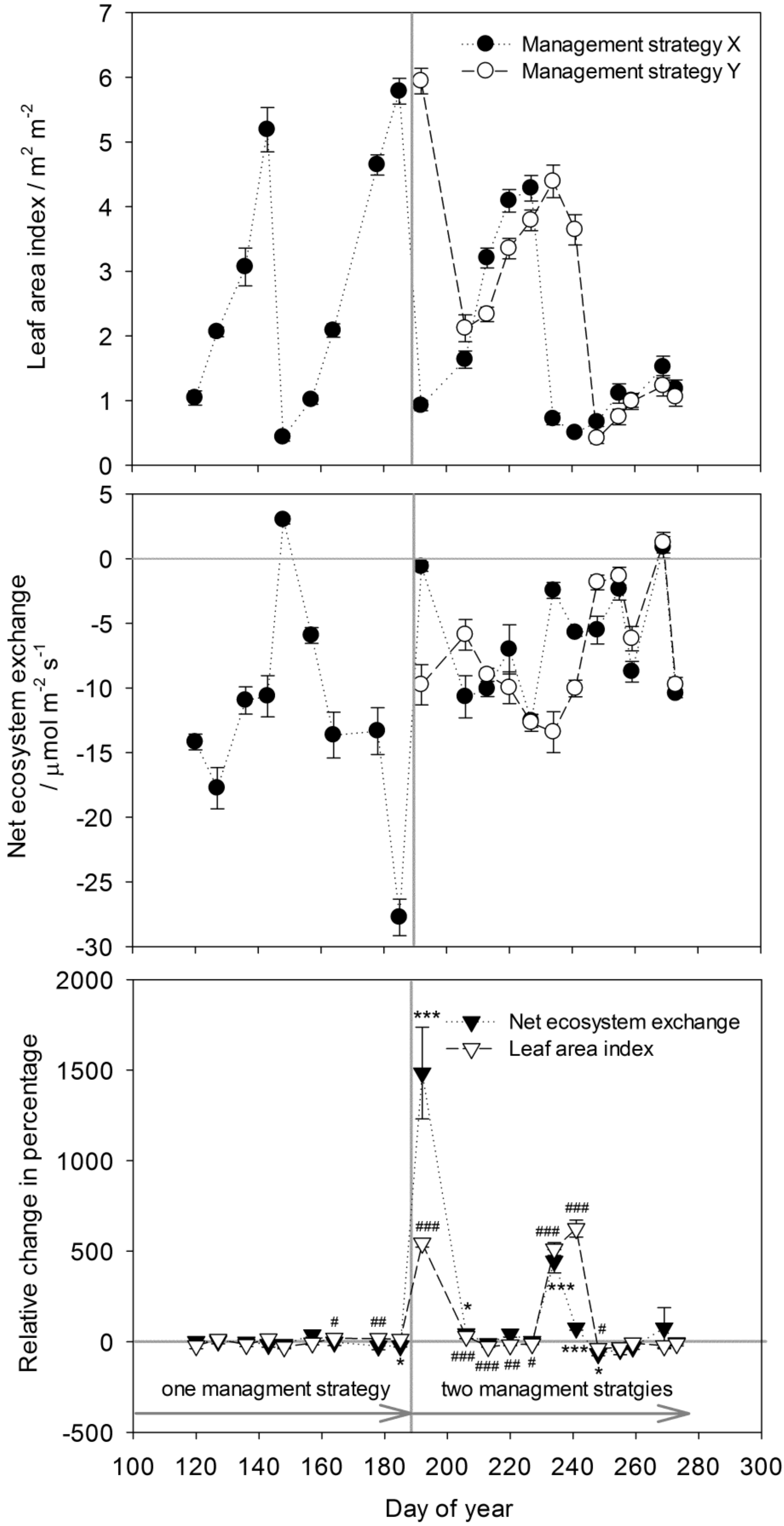

Management strategy X
Management strategy Y
Leaf area index / m2 m-2
Net ecosystem exchange / μmol m-2 s-1
Net ecosystem exchange
Leaf area index
Relative change in percentage
one managment strategy
two managment stratgies
Day of year

Figure 6: Relation between leaf area index and net ecosystem exchange. Data sets include values obtained at all 21 measurement sites where management strategy X was established (n=292; Table S-2, Supplementary data). Best fits are shown as solid line and respective equations are provided.